

Article

Graphene Oxide Nanoparticles and Their Influence on Chromatographic Separation Using Polymeric High Internal Phase Emulsions

Sidratul Choudhury ¹, Emer Duffy ¹, Damian Connolly ², Brett Paull ³ and Blánaid White ^{1,*}

¹ School of Chemical Sciences, Dublin City University, D09 W6Y4 Dublin, Ireland; sidratul.choudhury2@mail.dcu.ie (S.C.); emer.duffy@dcu.ie (E.D.)

² APC Ltd., Cherrywood Business Park, Loughlinstown, D18 DH50 Dublin, Ireland; damian.connolly@aprocess.com

³ Australian Centre for Research on Separation Science; ARC Centre of Excellence for Electromaterials Science, School of Physical Sciences, University of Tasmania, Hobart, 7001 TAS, Australia; brett.paull@utas.edu.au

* Correspondence: blanaid.white@dcu.ie; Tel.: +353-1-700-6731

Academic Editor: Zuzana Zajickova

Received: 8 December 2016; Accepted: 7 February 2017; Published: 11 February 2017

Abstract: This work presents the first instance of reversed-phase liquid chromatographic separation of small molecules using graphene oxide nanoparticle-modified polystyrene-divinylbenzene polymeric high internal phase emulsion (GONP PS-*co*-DVB polyHIPE) materials housed within a 200- μ m internal diameter (i.d.) fused silica capillary. The graphene oxide nanoparticle (GONP)-modified materials were produced as a potential strategy to increase both the surface area limitations and the reproducibility issues observed in monolithic stationary phase materials. GONP PS-*co*-DVB polyHIPEs were found to have a surface area up to 40% lower than unmodified polymeric high internal phase emulsion (polyHIPE) stationary phases. However, despite having a surface area significantly lower than that of the unmodified material, the GONP-modified polyHIPEs demonstrated superior analyte adsorption properties. Reducing the GONP material did not have any significant impact on elution order or retention factor of the analytes, which was most likely due to low GONP loading attributed to the 250-nm GONPs utilised. The lower surface area of GONP-modified polyHIPEs provided similar separation efficiency and increased repeatability from injection to injection resulting in % relative standard deviations (%RSDs) of less than 0.6%, indicating the potential offered by graphene oxide (GO)-modified polyHIPES in flow through applications such as adsorption or separation processes.

Keywords: polymeric high internal phase emulsion (polyHIPE); high internal phase emulsions; graphene oxide; liquid chromatography; nanoparticles; polystyrene; divinylbenzene; monolith; macroporous materials

1. Introduction

Polymeric high internal phase emulsions (polyHIPEs) are polymer materials which are formed from emulsions where the internal droplet phase has a ratio greater than 0.74 of the total emulsion volume. When the internal droplet phase is aqueous and the continuous phase is organic, upon polymerisation a monolithic structure results with the formation of interconnected pore structures [1–4]. The larger pore structures are known as voids while the smaller pore structures within the void are known as windows. PolyHIPEs have been successfully applied in areas such as electrochemistry [5], tissue engineering [6,7] and solid-phase extraction [8,9]. PolyHIPEs have been developed as stationary phase materials for standard-bore liquid chromatography applications,

as shown in particular in [10–13]. As polyHIPEs are macroporous materials (pores from 10 to 100 μm) they are ideal for biological separations and have been demonstrated previously in the literature [10,11,13]. However, fewer instances of small molecule separation using high performance liquid chromatography (HPLC) methods have been utilised [12].

Due to intrinsic large pore structures the surface area of these materials is very low, typically ranging from $3\text{ m}^2\cdot\text{g}^{-1}$ to $20\text{ m}^2\cdot\text{g}^{-1}$ [14]. Attempts to increase the surface area of these materials have consisted mainly of introducing different additional porogens, which can leave the materials with low mechanical rigidity [15,16]. This decreased rigidity would compromise the material's ability to function as a high pressure stationary phase. An alternative potential strategy is to incorporate an additional component into the polymerisation mixture to increase the surface area of the material [17]. Previously, polymer monoliths have been chemically modified to allow for nanoparticle (NP) attachment as a means to increase surface area [18,19]. However, the incorporation of NPs in polyHIPEs typically results in Pickering emulsions which generally form closed cell structures, making them unsuitable for use as chromatographic stationary phases [20].

Graphene oxide (GO) has been utilised in the fabrication of polymer materials such as for increasing the flame retardant ability of polymer materials for fire safety, demonstrating the importance of GO incorporation in material applications [21–25]. Graphene oxide nanoparticles (GONPs) are also amphiphilic, and are thus suitable for use as a Pickering agent to form an emulsion. Pickering studies using GO have resulted in the formation of polystyrene particles coated in GO and even hollow hybrid polymer GO particles [26–32]. The successful use of GONPs, particularly with emulsion polymerisation, enables the development of GONP-modified polyHIPE materials, potentially enhancing these materials in terms of stability and surface area. GONP materials have been applied as solid-phase extraction materials [33], progressing from the insoluble graphene solid-phase techniques that were being developed at the time. Due to the presence of oxygen, GONPs have greater solubility in various solvents, allowing an ideal adsorbent material for extraction of small molecules, bulky and aromatic compounds and large biomolecules [34–36]. A GONP/silica hybrid stationary phase aminated and functionalised with C18 ligands was one of the first instances in which GO was used in liquid chromatography; here the separations were dominated by π – π interactions. GONP-modified stationary phases resulted in changes of elution order of analytes including polyaromatic hydrocarbons (PAHs), anilines and phenols when compared to commercial C18 stationary phases [37]. Another GONP/silica hybrid stationary phase bonded with C18 ligands was modified with gold NPs and used in reverse-phase liquid chromatography (RP-HPLC) and hydrophilic interaction liquid chromatography (HILIC) for separation of isomeric dihydroxylbenzenes, alkylbenzenes, nucleosides and amino acids [38]. Additionally, the use of GONP-functionalised monoliths have also been demonstrated where GONPs were silanised and used as a crosslinker for the polymerisation of glycidyl methacrylate and ethylene glycol dimethacrylate [39]. The resulting monoliths were shown to separate mixtures of steroids as well as more polar analytes such as aromatic amines. In addition to utilising GO-modified stationary phases in liquid chromatography, the use of GO in stationary phases as conductive stationary phases is of increasing interest. Increased conductivity is generally achieved by the reduction of the GONPs with hydrazine hydrate, however the reduction is also possible using ascorbic acid. The enhanced conductive properties allow for interesting electrochemically functionalised separations. Such modifications have already been demonstrated in the separation of acid nitrophenol isomers, basic nitroaniline isomers, and neutral PAHs using open tubular capillary electrochromatography (OTCEC) [40]. To date however, polyHIPE modifications with GONPs have not been explored.

In this study GONPs measuring 250 nm in size were incorporated into polystyrene-divinylbenzene polymeric high internal phase emulsions (PS-*co*-DVB polyHIPEs) in an attempt to align the amphiphilic GONPs along the aqueous phase–organic phase interface while simultaneously retaining the open pore structure of the polyHIPE. A major limitation of polyHIPE materials is their low surface area. The addition of GONP was a hypothesised novel method to overcome this limitation. Resulting

novel GONP-modified polyHIPE chromatographic stationary phases were fabricated and successfully applied for the RPLC separation of alkylbenzenes. The GONP-modified columns were reduced in situ by flushing with ascorbic acid. Despite the modified materials having lower surface areas than the unmodified material, the GONP polyHIPEs showed comparable separation of alkylbenzenes to that of the higher surface area polyHIPE and superior separation to GONP/silica hybrid stationary phases in the literature [38].

2. Results and Discussion

2.1. Material Characterisation

PS-*co*-DVB polyHIPE materials were fabricated in situ within fused silica capillary housings. Scanning electron microscopy (SEM) imaging confirmed attachment of the polyHIPE to the capillary wall, as shown in Figure S1. No contraction or detachment from the capillary wall was observed after flow-through. Figure 1a shows the PS-*co*-DVB polyHIPE within fused silica capillary where no GONPs have been incorporated. However, Figure 1b shows the effect of the 250-nm GONPs on the polyHIPE structure. The GONP-modified polyHIPE appears to have a greater surface roughness compared to the unmodified material. It was expected that the GONP-modified material, upon application of Brauner–Emmet–Teller (BET) theory, would show an increase in surface area. However, the resulting information obtained through nitrogen adsorption/desorption showed that the surface area of the unmodified material was $25 \text{ m}^2 \cdot \text{g}^{-1}$ while the GONP-modified material was found to be only $16 \text{ m}^2 \cdot \text{g}^{-1}$. Upon fabrication of an additional GONP batch, in the repeat BET analysis the resulting surface area was found to be lower at $12 \text{ m}^2 \cdot \text{g}^{-1}$. The Barret–Joyner–Halenda (BJH) method was applied for investigation of pore size distributions, and revealed there was a reduction in mesopore size and volume with the addition of GONP to the material. The average mesopore width was calculated to be $\sim 20 \text{ nm}$ in PS-*co*-DVB polyHIPEs compared to $\sim 16 \text{ nm}$ in graphene oxide nanoparticle-modified polystyrene-divinylbenzene polymeric high internal phase emulsion (GONP PS-*co*-DVB polyHIPEs). Pore size distribution curves obtained from the absorption branch of the isotherm are included, with Figure S2 showing the BJH pore size distribution curve for the PS-*co*-DVB polyHIPE, and Figure S3 showing the same for the GONP PS-*co*-DVB polyHIPE. As evident from Figures S2 and S3, there was a broader width distribution in the material prior to addition of GONP. Following addition of GONP there was also a reduction in pore volume from $0.098 \text{ cm}^3 \cdot \text{g}^{-1}$ to $0.035 \text{ cm}^3 \cdot \text{g}^{-1}$. This shows a definite reduction in surface area and pore width and volume with the addition of GONPs, however it is argued that nitrogen adsorption on hydrophobic surfaces is less localised due to weaker adsorbate–surface interactions where there is more freedom for lateral movement. This can result in nitrogen molecules occupying a larger area and thus leads to an underestimation of the surface area of the hydrophobic surface since there are less nitrogen molecules in the adsorbed monolayer [41]. Therefore, the application of these polyHIPE materials in liquid chromatography was explored as a means to further understand their properties through the reversed phase separation of a series of hydrophobic alkylbenzenes.

The addition of NPs to polymer monoliths has been shown to negatively impact upon surface area [18,19,42], where the decrease is generally attributed to NPs blocking the pores of the monolithic materials. However, in the case of polyHIPEs which possess large macropores, this is an unlikely source of the reduction in surface area. The pore morphology was affected by addition of 250-nm GONPs to the emulsion, as observed by SEM imaging, where a reduction in both void and window size was noted, as shown in Table 1. This change in morphology was expected to impact upon the properties of the polyHIPE when applied as an adsorbent.

Table 1. Change in void and window size upon addition of graphene oxide nanoparticles (GONPs). PolyHIPE: polymeric high internal phase emulsion

PolyHIPE	Void Size (μm)	Window Size (μm)
Unmodified	15.59 ± 13.62	4.29 ± 1.73
Modified	10.92 ± 5.81	2.48 ± 0.75

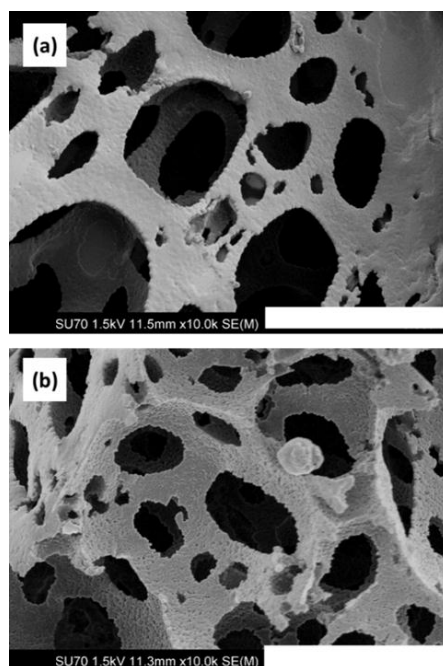


Figure 1. Field emission scanning electron microscope (FESEM) images showing (a) the unmodified polystyrene-divinylbenzene high internal phase emulsion (PS-co-DVB polyHIPE) and (b) the GONP-modified PS-co-DVB polyHIPE polymerised within fused silica capillary housings. Magnification of 10,000 \times and scale bar of 5 μm .

Figure 2 shows the Fourier transform infrared (FTIR) absorption spectrum of an unmodified polyHIPE. FTIR analysis demonstrated that on an unmodified polyHIPE no OH stretches present in the expected region of 3200–3600 cm^{-1} were observed.

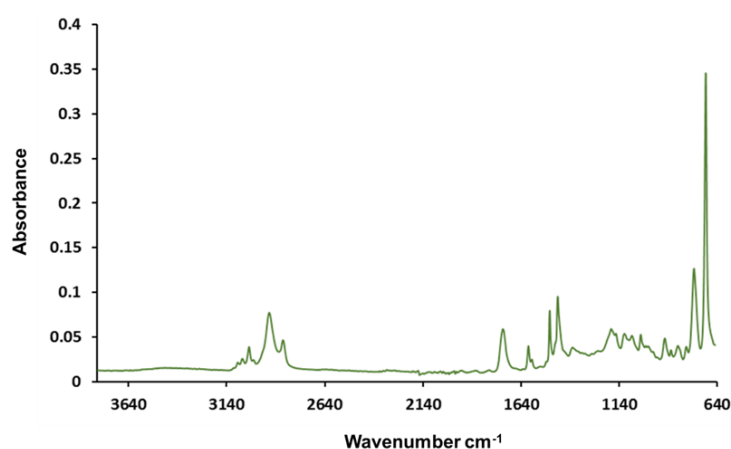


Figure 2. Fourier transform infrared (FTIR) absorption spectrum of an unmodified polyHIPE where no OH absorption region is observed.

Interestingly, when the GONP-modified polyHIPEs (#1, orange and #2, purple) were analysed using FTIR as shown in Figure 3, the 250-nm GONP polyHIPEs had an absorption profile where two distinct absorption peaks resulted in the OH region. The two peaks are typically observed when OH groups are present on a molecule surface and no hydrogen bonding can occur [43]. It was also noted that carbonyl absorption was observed in the FTIR results. This was expected, as the polyHIPE containing GONPs was expected to absorb in the region of 1720 cm^{-1} as graphene oxide contains multiple C=O groups; however, this absorption peak could also be attributable to the starting compound Span[®] 80. As shown in Figure S4, the C=O peak for Span[®] 80 was evident at 1740 cm^{-1} . FTIR spectra were also obtained on washing of Soxhlet extraction solvents methanol and water (shown in Figure S5), where there is absorption in the region of 1740 cm^{-1} in the MeOH Soxhlet extraction solvent. Therefore, the peak in Figure 2 at approx. 1740 cm^{-1} is likely attributable to Span[®] 80, and the equivalent peak in Figure 3 could mask a GONP C=O peak in this area. As both the starting material Span[®] 80 and the GONPs have C=O stretches, this compromises the assignment of any peaks observed in this region. For this reason, the presence of OH stretches in the region of $3200\text{--}3600\text{ cm}^{-1}$ more conclusively supports GONP incorporation, as these peaks are not observed in Figure 2, only Figure 3. There was no absorption peak observed at 1720 cm^{-1} for either of the GONP-containing polyHIPEs, which may also suggest that the GO may have been at least partially embedded within the polymeric material. That the GONPs did not protrude fully from the pore surface as expected, but instead partially embedded within the material, likely contributed to the lack of expected surface area increase. Partitioning is known to occur between emulsion phases [44] and is dependent on the surfactant layer at the interface [14]. Span[®] 80 is associated with insufficient packing in the interfacial film owing to the cis conformation of the oleic tail, which can lead to partitioning and GONPs embedding in the pore walls [45]. A similar effect has been reported for iron oxide NPs in dicyclopentadiene polyHIPEs, where the amount of NPs embedded in the polymer was found to be directly attributable to the volume of surfactant [46].

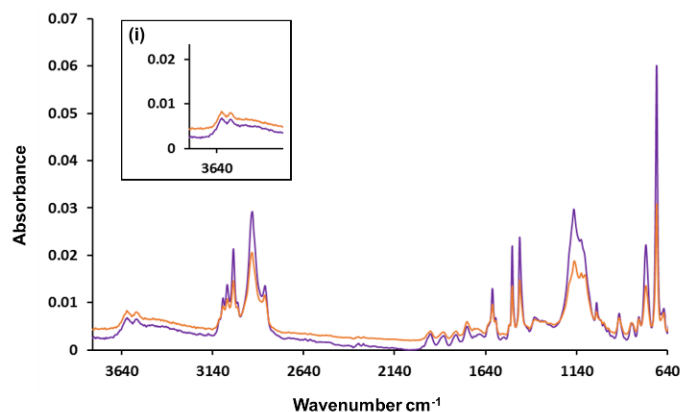


Figure 3. FTIR absorption spectra of GONP-modified polyHIPE #1 (orange) and GONP-modified polyHIPE #2 (purple) where (i) shows the OH absorption region.

2.2. Application of Graphene Oxide-Modified PolyHIPE Materials in Liquid Chromatographic Separations

The separation of alkylbenzenes on both unmodified PS-*co*-DVB and GONP-modified PS-*co*-DVB capillary columns of 229 mm length \times 200 μm internal diameter (i.d.) were achieved using isocratic reversed-phase liquid chromatography (RP-HPLC) separation as shown in Figure 4. It was expected that GONP-modified polyHIPEs would have a reduced retention time due to the hydrophilic groups present on the polyHIPE surface and the observed 36% decrease in surface area for the GONP-modified column. However, when statistically analysed, it was found at 95% confidence that there was no significant change observed in retention times. Given the decrease in surface area and reduction in

stationary phase interactions, the separation achieved by the GONP-modified column illustrated in Figure 3 shows a remarkable separation relative to the unmodified column.

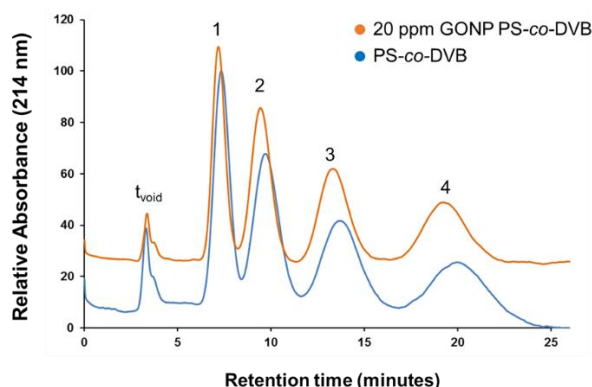


Figure 4. Isocratic alkylbenzene separation on 22.9 cm \times 200 μ m internal diameter (i.d.) capillary columns of a graphene oxide nanoparticle-modified polystyrene-divinylbenzene polymeric high internal phase emulsion (GONP PS-co-DVB9 column (orange) and PS-co-DVB polyHIPE (blue). Mobile phase 50:50 acetonitrile:water, sample concentration 0.5 mg·L⁻¹, injection volume 0.1 μ L, flow rate 5 μ L·min⁻¹, detection wavelength 214 nm. Analytes: ethylbenzene (1), propylbenzene (2), butylbenzene (3) and pentylbenzene (4). (t_{void} denotes time taken for void volume to reach the detector)

Despite the reduction in surface area, the modified material nonetheless achieved similar separation capacities (shown in Table 2), which are attributed to the changes in surface morphology and pore dimensions following addition of GONP. Previous reports, detailing hybrid GONP/silica stationary phases applied to the isocratic separation of alkylbenzenes failed to achieve a separation, where a co-elution of the target analytes was observed [38]. That the separation was maintained despite the significant reduction in surface area points to an enhanced separation mechanism for the GONP-modified material. It was hypothesised that the presence of GONPs and what we have established as a “popcorn effect” demonstrated in the morphology of these materials could have attributed to the superior adsorption of the analytes. This “popcorn effect” illustrated in the field emission scanning electron (FESEM) image of bulk-polymerised GONP-modified polyHIPE in Figure 5 below has also been observed in other GONP-modified polymers, showing that while the GONPs did not have a significant effect on the surface area of the polyHIPEs it did interestingly affect the overall morphology.

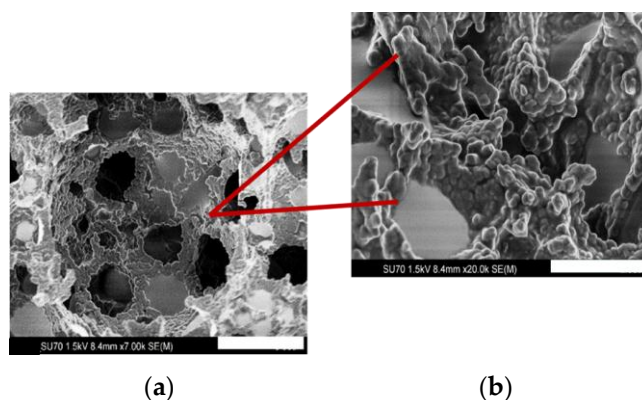


Figure 5. FESEM images of (a) GONP-modified PS-co-DVB polyHIPE polymerised in bulk at magnification of 7000 \times (scale bar 5 μ m) to show GONP-encapsulated morphology and (b) GONP coverage at 20,000 \times (scale bar 2 μ m).

Table 2. Separation performance characteristics of GONP-modified polyHIPEs and reduced GONP-modified polyHIPEs compared to unmodified polyHIPEs, $n = 3$. t_r : retention time (min); RSD (%): % relative standard deviation; R_s : Resolution; k' : Capacity factor.

Column	t_r (min)	RSD (%)	R_s	k'
Unmodified polyHIPE				
Ethylbenzene	7.27 ± 0.06	0.9	1.14	1.15 ± 0.02
Propylbenzene	9.62 ± 0.10	0.1	1.26	1.85 ± 0.02
Butylbenzene	13.48 ± 0.16	1.2	1.36	2.99 ± 0.05
Pentylbenzene	19.73 ± 0.21	1.2	2.09	4.85 ± 0.06
GONP-modified polyHIPE				
Ethylbenzene	6.94 ± 0.02	0.3	1.25	1.11 ± 0.01
Propylbenzene	9.11 ± 0.02	0.3	1.34	1.76 ± 0.01
Butylbenzene	12.80 ± 0.05	0.5	1.51	2.89 ± 0.02
Pentylbenzene	18.60 ± 0.10	0.6	1.91	4.65 ± 0.03
Reduced GONP-modified polyHIPE				
Ethylbenzene	7.13 ± 0.04	0.5	0.98	1.13 ± 0.03
Propylbenzene	9.38 ± 0.05	0.5	1.27	1.78 ± 0.01
Butylbenzene	13.26 ± 0.09	0.6	1.42	2.93 ± 0.03
Pentylbenzene	19.41 ± 0.06	0.3	1.66	4.73 ± 0.05

In addition to the superior adsorption effects observed, the retention time repeatability of both GONP columns was excellent, (%RSD 0.3%–1.2%), as shown in Table 2. These %RSD values were comparable to a similar separation observed in the literature using capillary electrochromatography (CEC) [47,48]. Additionally, resolution (R_s) between all analytes was greater than 1, meaning that all peaks could be differentiated easily. The polyHIPEs within capillary housing therefore have shown improved resolution, reduced retention times (t_r), and greater repeatability for the separation of alkylbenzenes, as compared to previous polyHIPE chromatographic separations.

2.3. Investigating the Reduction of Graphene Oxide-Modified PolyHIPE Stationary Phases

When the above column was reduced using ascorbic acid, it was expected that the retention time of the alkylbenzenes would increase. Reduction of GONPs should eliminate hydrophilic groups on the polyHIPE surface, and result in the formation of graphene. Graphene, being more hydrophobic than GONPs, was expected to improve analyte retention in the stationary phase through increased hydrophobic interactions. As shown in Figure 6, however, the peak shape and elution order of the separation remained similar to the previous separation and similar to alkylbenzene separations in the literature [49–53]. An increase in retention time was observed as compared to the GONP polyHIPE, which can be linked to increased hydrophobic interactions between the analytes and the reduced stationary phase, however, this increase was small as a result of the low loading of GONP in the initial emulsion. Upon increased addition of GONPs to the precursor emulsion during preparation of polyHIPEs, an unstable emulsion resulted, which is attributed to the relatively large size (250 nm) of the GO sheets [31]. Future studies will focus on the incorporation of smaller GONPs, which are anticipated to provide a more accessible functionalised surface for improved analyte-stationary phase interaction, and should result in a superior chromatographic performance [31,32]. The larger GONPs utilised herein were likely at least embedded within the internal structure of the polymer backbone. Electrolyte concentration has also been shown to influence the stability of GONP suspensions within an emulsion, and should be further optimised to allow the optimal GONP dimension and loading to be determined [31].

An increase in intra-injection repeatability was observed, resulting in %RSD as low as 0.3% following the reduction step. These %RSD values (Table 2) were comparable to those observed in similar separations in the literature [49–53]. Despite the minimal variation observed in retention times and small reduction in R_s values, the injection repeatability was excellent with respect to the variability,

which is expected with monolithic columns [54]. Furthermore, the modified polyHIPE material, with a lower surface area, maintained a good separation performance, thus highlighting the potential of further developing nanoparticle-modified polyHYPES for applications in adsorption. The ease of tailoring for these materials is a distinct advantage, and a variety of nanomaterials could potentially be incorporated provided their dispersion quality is sufficient.

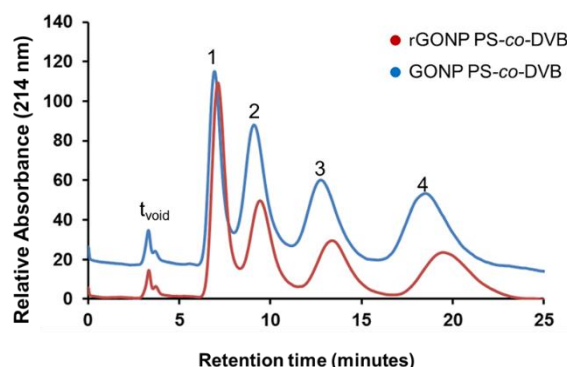


Figure 6. Isocratic alkylbenzene separation on 22.9 cm \times 200 μ m i.d. capillary columns of a reduced graphene oxide nanoparticle (rGONP) PS-co-DVB column (red) and PS-co-DVB polyHIPE (blue). Mobile phase 50:50 acetonitrile:water, sample concentration 0.5 mg·L⁻¹, injection volume 0.1 μ L, flow rate 5 μ L·min⁻¹, and detection wavelength 214 nm. Analytes noted as ethylbenzene (1), propylbenzene (2), butylbenzene (3) and pentylbenzene (4). (t_{void} denotes time taken for void volume to reach the detector).

Future work will involve a GONP loading study to investigate GONP loading as a result of a variety of initial concentrations, supported with additional characterisation approaches to enrich understanding of the resultant group of composites. This will be accompanied by optimisation to ensure homogenous dispersion of NPs in polyHYPES, in addition to investigations of alternative carbonaceous materials (reviewed in [42]) to meet the overall goals of our research.

3. Materials and Methods

Millipore ultrapure water purified to a resistance of > 18 M Ω ·cm was used throughout. Styrene \geq 99%, divinylbenzene 80%, calcium dihydrochloride > 99% and Span[®] 80, ethylbenzene > 99.8%, propylbenzene > 99%, butylbenzene > 99%, pentylbenzene 99% and ascorbic acid >99% were purchased from Sigma-Aldrich, Castle Hill, New South Wales, Australia. Alkylbenzene stock standards and working standards were prepared at 100 mg·L⁻¹ and 0.5 mg·L⁻¹ in acetonitrile respectively. All solvents were used as received and were of analytical HPLC grade. An aqueous suspension of graphene oxide nanoparticles (GONPs; 2 mg·mL⁻¹) was donated by the University of Wollongong and was used as received. A Zetasizer Nano ZS particle analyser from ATA Scientific (Taren Point, NSW, Australia) fitted with a 632.8 nm red laser and a 175° backscatter detector was used to estimate the particle size distribution of GO suspensions. The average sheet size of GO in suspension was found to be 249.8 nm (particle size distribution data are shown in Figure S6). Fused silica capillaries of 200- μ m internal diameter were purchased from Polymicro Technologies, Phoenix, AZ, USA.

3.1. Silanisation of Fused Silica Capillary

Fused silica capillaries were washed with acetone (5 min, 1 μ L·min⁻¹), dried with nitrogen (10 min) and then flushed sequentially with 0.2 M NaOH (30 min, 1 μ L·min⁻¹), water (5 min, 1 μ L·min⁻¹) and 0.2 M HCl (5 min, 1 μ L·min⁻¹) before further drying with a nitrogen flow for 20 min. The capillary was filled with 50% (v/v) 3-(trimethoxysilyl) propyl methacrylate in acetone, sealed and incubated at 60 °C in a water bath for 48 h. Finally, the capillary was rinsed with acetone (5 min, 1 μ L·min⁻¹) and dried with nitrogen.

3.2. Fabrication of Graphene Oxide-Modified PolyHIPE Capillary Columns

PS-*co*-DVB polyHIPEs were prepared based on a modified procedure described by Tunç et al. [47]. Briefly, for a 90% polyHIPE the emulsion consisted of two separately prepared phases: the aqueous phase (15 mL H₂O, 0.03 g potassium persulfate (PPS), 0.01 g calcium chloride dihydrate), and the organic phase (1.33 mL styrene, 0.33 mL divinylbenzene, 0.33 g Span[®] 80). The organic phase was stirred under nitrogen in a 250-mL round-bottomed flask with an overhead stirrer at 320 rpm and the aqueous phase was added drop-wise using a hypodermic syringe. When all of the aqueous phase was added to the emulsion, it was stirred for 20 min. A similar procedure was followed in preparation of the emulsion for GONP-modified polyHIPEs which are referred to throughout as GONP PS-*co*-DVB polyHIPEs. Following the dropwise addition of aqueous phase, 150 µL of the 2 mg·mL^{−1} GONP suspension was added dropwise into the emulsion and it was stirred for 20 min. Emulsions were then transferred by syringe into the silanised fused silica capillaries using an upward flow direction to eliminate unwanted air-bubbles or voids throughout the housing. Columns were incubated at 60 °C for 48 h, after which they were washed with methanol at 10 µL·min^{−1} for 24 h.

3.3. Reduction of Graphene Oxide-Modified PolyHIPE Capillary Columns

GONP-modified PS-*co*-DVB polyHIPE columns were fabricated within fused silica capillary as described previously [55]. These columns were reduced using a syringe pump flowing a solution of 2 mM ascorbic acid at 0.3 µL·min^{−1} for 1 h. The column was washed with water for 30 min and then with methanol for 1 h before using for separation of alkylbenzenes. This procedure was also repeated with an unmodified PS-*co*-DVB polyHIPE column to use as a control. Following the reduction step, the adsorbents were referred to as reduced graphene oxide nanoparticle (rGONP) PS-*co*-DVB polyHIPE.

3.4. Instrumental Conditions

High resolution imaging was carried out using a Hitachi SU-70 field emission scanning electron microscope (FESEM) (Hitachi, Maidenhead, UK) with Image J software for image processing. All samples were gold sputtered using a BalTec SCD 050 sputter coater (Ladd Research, 83 Holly Ct, Williston, VT, USA) prior to imaging at 1.5 kV. Surface areas were characterised by the nitrogen adsorption/desorption method using a Micromeritics Gemini TriStar surface area analyser (Micromeritics, Norcross, GA, USA). The balance used was a Sartorius Extend (Sartorius, Goettingen, Germany) and the sonication bath used was from Branson Ultrasonic Corporation (Danbury, CT, USA). FTIR analysis was carried out using a Bruker IFS 66 infrared spectrometer. An Ultimate 3000 capillary chromatography system (Thermo Fisher Scientific, Sunnyvale, CA, USA) was used to acquire all chromatographic data. The dimensions of polyHIPE columns used in silicosteel tubing were 229 mm × 200 µm i.d. The RP-HPLC separations were performed under the following conditions: the mobile phase was 50:50 acetonitrile/water, the flow rate was 5 µL·min^{−1} with an injection volume of 1 µL, column temperature was 25 °C and ultraviolet (UV) detection was at 214 nm.

4. Conclusions

In this study the successful chromatographic separation of alkylbenzenes utilising novel GONP-modified polyHIPE materials has been demonstrated. The observed changes in retention time for alkylbenzenes on GONP and rGONP polyHIPE materials correspond with the lower surface area of these adsorbents determined through application of BET theory, and highlight a potential route towards improving the efficiency of these materials by improving their morphology and functionality without the necessity of dramatically increasing their surface area.

In addition, the injection to injection replication of both columns prior to and post reduction were exceptional with respect to the variability which is expected with monolithic columns. The resulting separations provided an understanding of these materials during their development and have

presented an opportunity to further explore these materials in flow-through applications in areas such as adsorption/separation processes, and following suitable functionalisation, in catalysis.

Supplementary Materials: The following are available online at <http://www.mdpi.com/2297-8739/4/1/5/s1>.

Acknowledgments: The authors would like to acknowledge the MASK Marie Curie IRES and the Irish Research Council (Grant number RS/2012/24) is gratefully acknowledged. In addition, the authors would like to acknowledge the assistance of Karsten Goemann, Sandrin Feig and Thomas Rodemann at the Central Science Laboratory in the University of Tasmania for FESEM and FTIR support.

Author Contributions: Sidratul Choudhury, Brett Paull and Blánaid White conceived and designed the experiments; Sidratul Choudhury and Emer Duffy performed the experiments; Sidratul Choudhury, Emer Duffy, Damian Connolly, Brett Paull and Blánaid White analysed the data; Sidratul Choudhury and Emer Duffy wrote the paper; Damian Connolly, Brett Paull and Blánaid White contributed as manuscript advisors. Each contributor was essential to the production of this work.

Conflicts of Interest: The authors declare no conflict of interest.

Abbreviations

i.d.	Internal diameter
RSD	Relative standard deviation
RP-HPLC	Reversed-phase high performance liquid chromatography
PS	Polystyrene
DVB	Divinylbenzene
GO	Graphene oxide
GONP	Graphene oxide nanoparticle
rGONP	Reduced graphene oxide nanoparticle
NP	Nanoparticles
SEM	Scanning electron microscopy
FESEM	Field emission scanning electron microscopy
FTIR	Fourier transform infrared spectroscopy
OTCEC	Open tubular capillary electrochromatography
CEC	Capillary electrochromatography
PAH	Polycyclic aromatic hydrocarbon
polyHIPE	polymeric high internal phase emulsion
PPS	Potassium persulfate
UV	Ultraviolet

References

1. Silverstein, M.S. Emulsion-templated porous polymers: A retrospective perspective. *Polymer* **2014**, *55*, 304–320. [[CrossRef](#)]
2. Choudhury, S.; Connolly, D.; White, B. Supermacroporous polyHIPE and cryogel monolithic materials as stationary phases in separation science: A review. *Anal. Meth.* **2015**, *7*, 6967–6982. [[CrossRef](#)]
3. Kimmins, S.D.; Cameron, N.R. Functional Porous Polymers by Emulsion Templating: Recent Advances. *Adv. Mater.* **2011**, *21*, 211–225. [[CrossRef](#)]
4. Pulko, I.; Krajnc, P. High Internal Phase Emulsion Templating—A Path to Hierarchically Porous Functional Polymers. *Macromol. Rapid Commun.* **2012**, *33*, 1731–1746. [[CrossRef](#)] [[PubMed](#)]
5. Silverstein, M.S.; Tai, H.; Sergienko, A.; Lumelsky, Y.; Pavlovsky, S. PolyHIPE: IPNs, hybrids, nanoscale porosity, silica monoliths and ICP-based sensors. *Polymer* **2005**, *46*, 6682–6694. [[CrossRef](#)]
6. Krenkova, J.; Foret, F.; Svec, F. Less common applications of monoliths: V. Monolithic scaffolds modified with nanostructures for chromatographic separations and tissue engineering. *J. Sep. Sci.* **2012**, *35*, 1266–1283. [[CrossRef](#)] [[PubMed](#)]
7. Barbetta, A.; Dentini, M.; Zannoni, E.M.; De Stefano, M.E. Tailoring the Porosity and Morphology of Gelatin-Methacrylate PolyHIPE Scaffolds for Tissue Engineering Applications. *Langmuir* **2005**, *21*, 12333–12341. [[CrossRef](#)] [[PubMed](#)]

8. Du, F.; Zhen, X.; Sun, L.; Qin, Q.; Guo, L.; Ruan, G. Development and validation of polymerized high internal phase emulsion monoliths coupled with high-performance liquid chromatography and fluorescence detection for the determination of trace tetracycline antibiotics in environmental water samples. *J. Sep. Sci.* **2015**, *38*, 3774–3780. [[CrossRef](#)] [[PubMed](#)]
9. Su, R.; Ruan, G.; Nie, H.; Xie, T.; Zheng, Y.; Du, F.; Li, J. Development of high internal phase emulsion polymeric monoliths for highly efficient enrichment of trace polycyclic aromatic hydrocarbons from large-volume water samples. *J. Chromatogr. A* **2015**, *1405*, 23–31. [[CrossRef](#)] [[PubMed](#)]
10. Yang, J.; Yang, G.L.; Liu, H.Y.; Bai, L.G.; Zhang, Q.X. Novel Porous Monolithic Column Using Poly(high internal phase emulsion) Methacrylate as Materials for Immunoglobulin Separation Performance on HPLC. *Chin. J. Chem.* **2010**, *28*, 229–234. [[CrossRef](#)]
11. Yao, C.H.; Qi, L.; Jia, H.Y.; Xin, P.Y.; Yang, G.L.; Chen, Y. A novel glycidyl methacrylate-based monolith with sub-micron skeletons and well-defined macropores. *J. Mater. Chem.* **2009**, *19*, 767–772. [[CrossRef](#)]
12. Choudhury, S.; Connolly, D.; White, B. Application of polymeric high-internal-phase-emulsion-coated stationary-phase columns in open-tubular capillary electrochromatography. *J. Appl. Polym. Sci.* **2016**, *133*, 11563–11568. [[CrossRef](#)]
13. Yao, C.H.; Qi, L.; Yang, G.L.; Wang, F.Y. Preparation of sub-micron skeletal monoliths with high capacity for liquid chromatography. *J. Sep. Sci.* **2010**, *33*, 475–483. [[CrossRef](#)] [[PubMed](#)]
14. Barbetta, A.; Cameron, N.R. Morphology and surface area of emulsion-derived (PolyHIPE) solid foams prepared with oil-phase soluble porogenic solvents: Span 80 as surfactant. *Macromolecules* **2004**, *37*, 3188–3201. [[CrossRef](#)]
15. Sergienko, A.Y.; Tai, H.W.; Narkis, M.; Silverstein, M.S. Polymerized high internal phase emulsions containing a porogen: Specific surface area and sorption. *J. Appl. Polym. Sci.* **2004**, *94*, 2233–2239. [[CrossRef](#)]
16. Cameron, N.R.; Barbetta, A. The influence of porogen type on the porosity, surface area and morphology of poly(divinylbenzene) PolyHIPE foams. *J. Mater. Chem.* **2000**, *10*, 2466–2471. [[CrossRef](#)]
17. Mert, E.H.; Kaya, M.A.; Yildirim, H. Preparation and Characterization of Polyester-Glycidyl Methacrylate PolyHIPE Monoliths to Use in Heavy Metal Removal. *Des. Monomers Polym.* **2012**, *15*, 113–126. [[CrossRef](#)]
18. Floris, P.; Twamley, B.; Nesterenko, P.N.; Paull, B.; Connolly, D. Fabrication and characterisation of gold nano-particle modified polymer monoliths for flow-through catalytic reactions and their application in the reduction of hexacyanoferrate. *Microchim. Acta* **2014**, *181*, 249–256. [[CrossRef](#)]
19. Floris, P.; Twamley, B.; Nesterenko, P.N.; Paull, B.; Connolly, D. Agglomerated polymer monoliths with bimetallic nano-particles as flow-through micro-reactors. *Microchim. Acta* **2012**, *179*, 149–156. [[CrossRef](#)]
20. Colver, P.J.; Bon, S.A.F. Cellular polymer monoliths made via pickering high internal phase emulsions. *Chem. Mater.* **2007**, *19*, 1537–1539. [[CrossRef](#)]
21. Gui, H.; Xu, P.; Hu, Y.; Wang, J.; Yang, X.; Bahader, A.; Ding, Y. Synergistic effect of graphene and an ionic liquid containing phosphonium on the thermal stability and flame retardancy of polylactide. *RSC Adv.* **2015**, *5*, 27814–27822. [[CrossRef](#)]
22. Yu, B.; Shi, Y.; Yuan, B.; Qiu, S.; Xing, W.; Hu, W.; Song, L.; Lo, S.; Hu, Y. Enhanced thermal and flame retardant properties of flame-retardant-wrapped graphene/epoxy resin nanocomposites. *J. Mater. Chem. A* **2015**, *3*, 8034–8044. [[CrossRef](#)]
23. Hu, W.; Yu, B.; Jiang, S.-D.; Song, L.; Hu, Y.; Wang, B. Hyper-branched polymer grafting graphene oxide as an effective flame retardant and smoke suppressant for polystyrene. *J. Hazard. Mater.* **2015**, *300*, 58–66. [[CrossRef](#)] [[PubMed](#)]
24. Zhou, K.; Yang, W.; Tang, G.; Wang, B.; Jiang, S.; Hu, Y.; Gui, Z. Comparative study on the thermal stability, flame retardancy and smoke suppression properties of polystyrene composites containing molybdenum disulfide and graphene. *RSC Adv.* **2013**, *3*, 25030–25040. [[CrossRef](#)]
25. Yu, B.; Wang, X.; Qian, X.; Xing, W.; Yang, H.; Ma, L.; Lin, Y.; Jiang, S.; Song, L.; Hu, Y.; et al. Functionalized graphene oxide/phosphoramidate oligomer hybrids flame retardant prepared via in situ polymerization for improving the fire safety of polypropylene. *RSC Adv.* **2014**, *4*, 31782–31794. [[CrossRef](#)]
26. Teo, G.H.; Ng, Y.H.; Zetterlund, P.B.; Thickett, S.C. Factors influencing the preparation of hollow polymer-graphene oxide microcapsules via Pickering miniemulsion polymerization. *Polymer* **2015**, *63*, 1–9. [[CrossRef](#)]
27. Thickett, S.C.; Zetterlund, P.B. Graphene oxide (GO) nanosheets as oil-in-water emulsion stabilizers: Influence of oil phase polarity. *J. Colloid Interface Sci.* **2015**, *442*, 67–74. [[CrossRef](#)] [[PubMed](#)]

28. Man, S.H.C.; Thickett, S.C.; Whittaker, M.R.; Zetterlund, P.B. Nano-sized graphene oxide as sole surfactant in miniemulsion polymerization for nanocomposite synthesis: Effect of pH and ionic strength. *Polymer* **2014**, *55*, 3490–3497. [[CrossRef](#)]
29. Man, S.H.C.; Thickett, S.C.; Whittaker, M.R.; Zetterlund, P.B. Synthesis of polystyrene nanoparticles “armoured” with nanodimensional graphene oxide sheets by miniemulsion polymerization. *J. Polym. Sci. A Polym. Chem.* **2013**, *51*, 47–58. [[CrossRef](#)]
30. Man, S.H.C.; Yusof, N.Y.M.; Whittaker, M.R.; Thickett, S.C.; Zetterlund, P.B. Influence of monomer type on miniemulsion polymerization systems stabilized by graphene oxide as sole surfactant. *J. Polym. Sci. A Polym. Chem.* **2013**, *51*, 5153–5162. [[CrossRef](#)]
31. Thickett, S.C.; Zetterlund, P.B. Functionalization of Graphene Oxide for the Production of Novel Graphene-Based Polymeric and Colloidal Materials. *Curr. Org. Chem.* **2013**, *17*, 956–974. [[CrossRef](#)]
32. Thickett, S.C.; Zetterlund, P.B. Preparation of Composite Materials by Using Graphene Oxide as a Surfactant in Ab Initio Emulsion Polymerization Systems. *ACS Macro Lett.* **2013**, *2*, 630–634. [[CrossRef](#)]
33. Sitko, R.; Zawisza, B.; Malicka, E. Graphene as a new sorbent in analytical chemistry. *TrAC Trends Anal. Chem.* **2013**, *51*, 33–43. [[CrossRef](#)]
34. Liu, Q.; Shi, J.; Jiang, G. Application of graphene in analytical sample preparation. *TrAC Trends Anal. Chem.* **2012**, *37*, 1–11. [[CrossRef](#)]
35. Liu, Q.; Shi, J.; Sun, J.; Thanh, W.; Zeng, L.; Jiang, G. Graphene and Graphene Oxide Sheets Supported on Silica as Versatile and High-Performance Adsorbents for Solid-Phase Extraction. *Angew. Chem. Int. Ed.* **2011**, *50*, 5913–5927. [[CrossRef](#)] [[PubMed](#)]
36. Zhang, S.; Du, Z.; Li, G. Layer-by-Layer Fabrication of Chemical-Bonded Graphene Coating for Solid-Phase Microextraction. *Anal. Chem.* **2011**, *83*, 7531–7541. [[CrossRef](#)] [[PubMed](#)]
37. Liang, X.; Liu, S.; Song, X.; Zhu, Y.; Jiang, S. Layer-by-layer self-assembled graphene oxide/silica microsphere composites as stationary phase for high performance liquid chromatography. *Analyst* **2012**, *137*, 5237–5244. [[CrossRef](#)] [[PubMed](#)]
38. Liang, X.; Wang, X.; Ren, H.; Jiang, S.; Wang, L.; Liu, S. Gold nanoparticle decorated graphene oxide/silica composite stationary phase for high-performance liquid chromatography. *J. Sep. Sci.* **2014**, *37*, 1371–1379. [[CrossRef](#)] [[PubMed](#)]
39. Li, Y.; Qi, L.; Ma, H. Preparation of porous polymer monolithic column using functionalized graphene oxide as a functional crosslinker for high performance liquid chromatography separation of small molecules. *Analyst* **2013**, *138*, 5470–5478. [[CrossRef](#)] [[PubMed](#)]
40. Liu, X.L.; Liu, X.; Guo, L.P.; Yang, L.; Wang, S.T. Graphene oxide and reduced graphene oxide as novel stationary phases via electrostatic assembly for open-tubular capillary electrochromatography. *Electrophoresis* **2013**, *34*, 1869–1876. [[CrossRef](#)] [[PubMed](#)]
41. Zhaoxia, L. The Effect of Adsorbent Geometry and Surface Chemistry on HPLC Retention. Ph.D. Thesis, Setton Hall University, South Orange, NJ, USA, 2009.
42. Nesterenko, E.P.; Nesterenko, P.N.; Connolly, D.; He, X.; Floris, P.; Duffy, E.; Paull, B. Nano-particle modified stationary phases for high-performance liquid chromatography. *Analyst* **2013**, *138*, 4229–4254. [[CrossRef](#)] [[PubMed](#)]
43. Innocenzi, P. Infrared spectroscopy of sol-gel derived silica-based films: A spectra-microstructure overview. *J. Non-Cryst. Solids* **2003**, *316*, 309–319. [[CrossRef](#)]
44. Carnahan, E.J.; Bokhari, M.; Przyborski, S.A.; Cameron, N.R. Tailoring the morphology of emulsion-templated porous polymers. *Soft Matter* **2006**, *2*, 608–616. [[CrossRef](#)]
45. Barbetta, A.; Cameron, N.R.; Cooper, S.J. High internal phase emulsions (HIPEs) containing divinylbenzene and 4-vinylbenzyl chloride and the morphology of the resulting polyHIPE materials. *Chem. Commun.* **2000**, *3*, 221–222. [[CrossRef](#)]
46. Kovacic, S.; Matsko, N.B.; Ferk, G.; Slugovc, C. Nanocomposite foams from iron oxide stabilized dicyclopentadiene high internal phase emulsions: Preparation and bromination. *Acta Chim. Slov.* **2014**, *61*, 208–214. [[PubMed](#)]
47. Tunc, Y.; Gogelioglu, C.; Tuncel, A.; Ulubayram, K. Polystyrene-Based High Internal Phase Emulsion Polymer Monolithic Stationary Phase for Capillary Electrochromatography. *Sep. Sci. Technol.* **2012**, *47*, 2444–2449.

48. Tunc, Y.; Golgelioglu, C.; Hasirci, N.; Ulubayram, K.; Tuncel, A. Acrylic-based high internal phase emulsion polymeric monolith for capillary electrochromatography. *J. Chromatogr. A* **2010**, *1217*, 1654–1659. [[CrossRef](#)] [[PubMed](#)]
49. Urban, J.; Svec, F.; Frechet, J.M.J. Efficient Separation of Small Molecules Using a Large Surface Area Hypercrosslinked Monolithic Polymer Capillary Column. *Anal. Chem.* **2010**, *82*, 1621–1623. [[CrossRef](#)] [[PubMed](#)]
50. Urban, J.; Svec, F.; Frechet, J.M.J. Hypercrosslinking: New approach to porous polymer monolithic capillary columns with large surface area for the highly efficient separation of small molecules. *J. Chromatogr. A* **2010**, *1217*, 8212–8221. [[CrossRef](#)] [[PubMed](#)]
51. Tchaplal, A.; Colin, H.; Guiochon, G. Linearity of homologous series retention plots in reversed phase liquid chromatography. *Anal. Chem.* **1984**, *56*, 621–625. [[CrossRef](#)]
52. Wang, Q.C.; Švec, F.; Fréchet, J.M.J. Reversed-phase chromatography of small molecules and peptides on a continuous rod of macroporous poly (styrene-co-divinylbenzene). *J. Chromatogr. A* **1994**, *669*, 230–235. [[CrossRef](#)]
53. Yang, J.; Yang, G.; Liu, H.; Bai, L.; Zhang, Q. Preparation and characterization of porous poly(vinyl ester) resin monoliths as separation media. *J. Appl. Polym. Sci.* **2011**, *119*, 412–418. [[CrossRef](#)]
54. Svec, F.; Huber, C.G. Monolithic materials: Promises, challenges, achievements. *Anal. Chem.* **2006**, *78*, 2100–2107. [[CrossRef](#)]
55. Fernandez-Merino, M.J.; Guardia, L.; Paredes, J.I.; Villar-Rodil, S.; Solis-Fernandez, P.; Martinez-Alonso, A.; Tascon, J.M.D. Vitamin C Is an Ideal Substitute for Hydrazine in the Reduction of Graphene Oxide Suspensions. *J. Phys. Chem. C* **2010**, *114*, 6426–6432. [[CrossRef](#)]



© 2017 by the authors; licensee MDPI, Basel, Switzerland. This article is an open access article distributed under the terms and conditions of the Creative Commons Attribution (CC BY) license (<http://creativecommons.org/licenses/by/4.0/>).